Temporal Variability Largely Explains Difference in Top-down and Bottom-up Estimates of Methane Emissions from a Natural Gas Production Region

Timothy L. Vaughn[a*], Clay S. Bell[a], Cody K. Pickering[a], Stefan Schwietzke[b,c], Garvin A. Heath[d,e] Gabrielle Pétron[b,c], Daniel Zimmerle[a*], Russell C. Schnell[c], Dag Nummedal[f]

[a] Colorado State University, Energy Institute and Mechanical Engineering, 430 N College, Fort Collins, CO 80524, USA

[b] University of Colorado Boulder, Cooperative Institute for Research in Environmental Sciences, 216 UCB, Boulder, CO 80309, USA

[c] NOAA ESRL Global Monitoring Division, 325 Broadway, Boulder, CO 80305, USA

[d] National Renewable Energy Laboratory, 15013 Denver West Parkway, Golden, CO 80401, USA

[e] Joint Institute for Strategic Energy Analysis, 15013 Denver West Parkway, Golden, CO 80401, USA

[f] Former Director, Colorado Energy Research Institute (retired), Colorado School of Mines, Golden, CO

*email: dan.zimmerle@colostate.edu, tim.vaughn@colostate.edu

Contents

S1 BU Results Summary Figures

Summary figures of BU model results are presented for the periods corresponding to TD flight windows on October 1st and 2nd in sections S1.1, and S1.2, respectively. Shown in each figure (from top to bottom) are: the spatial distribution of methane emissions within the study area; simulated BU longitudinal emission rate profiles, in total with 95% confidence intervals shown, and by category without confidence intervals; aggregate BU emissions for the western, eastern and total study area; the count of active manual liquid unloadings in the western and eastern portions of the study area.

The top panel in each figure shows the spatial distribution of methane emissions within the study area (150 km east-west, 65 km north-south) on a 0.04° longitudinal grid (∼3.8 km), colored by the emission intensity within each grid cell. The division between eastern and western portions of the study area at -92.1° longitude is also shown.

Simulated BU longitudinal emission rate profiles are shown in the second- and third-from-top panels. The second panel compares TD and BU profiles including 95% confidence intervals, while the third panel shows emission contributions by category. Emission contributions from natural gas sources in the production, gathering, and transmission sectors are shown, along with non-natural gas emissions from livestock, geologic seeps, and wetlands. Emissions from the natural gas distribution sector, rice cultivation, landfills, wastewater treatment, and other source categories contributing less than 1% each to the hourly BU average are omitted for clarity.

Finally, the bottom panel shows aggregate TD and BU emission estimates with 95% confidence intervals for the western and eastern portions of the study area, and the entire study area. The number of active manual liquid unloadings are tabulated for the western and eastern portions of the study area.

S1.1 BU Results Summary October 1st Flight Window

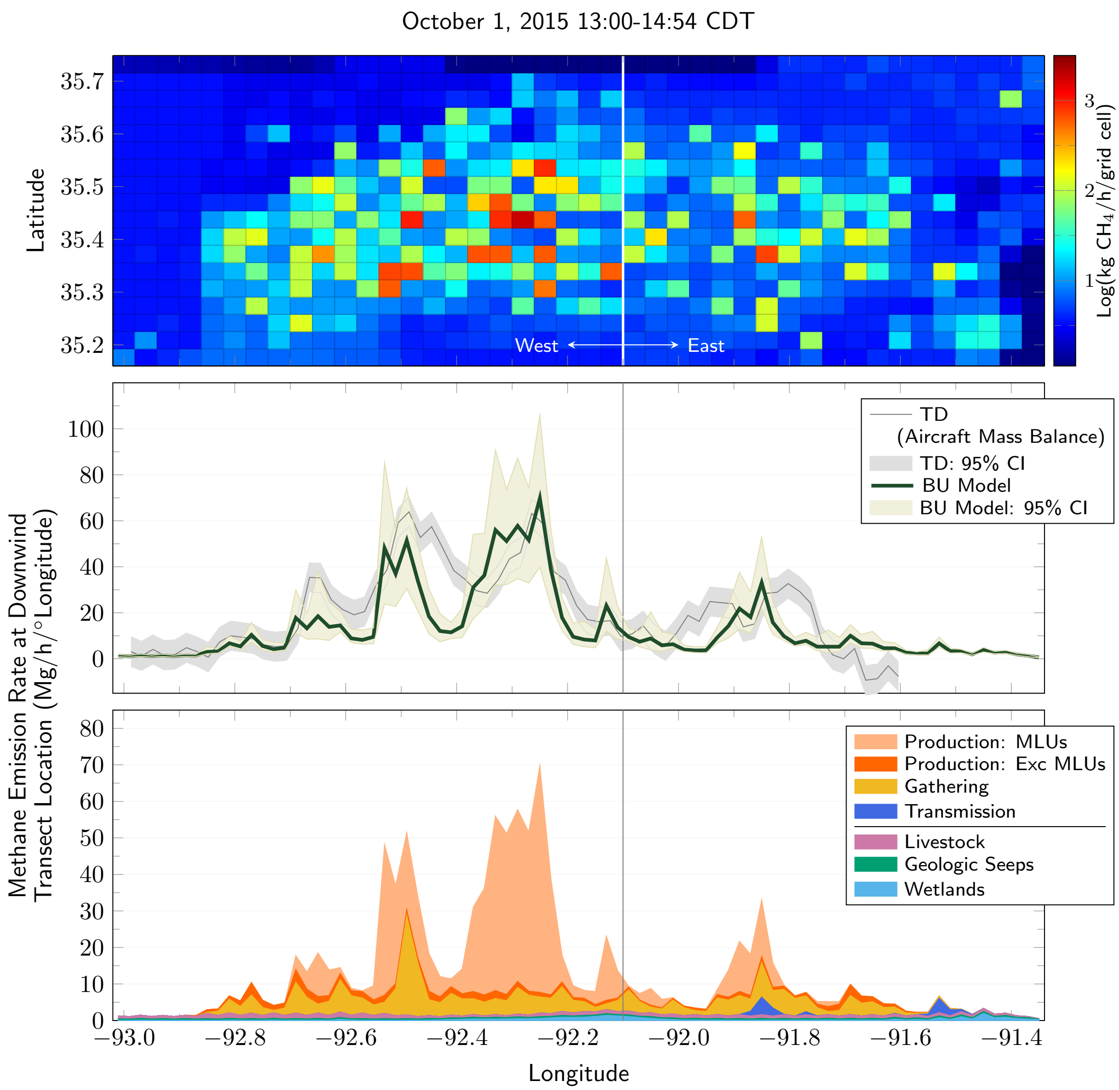

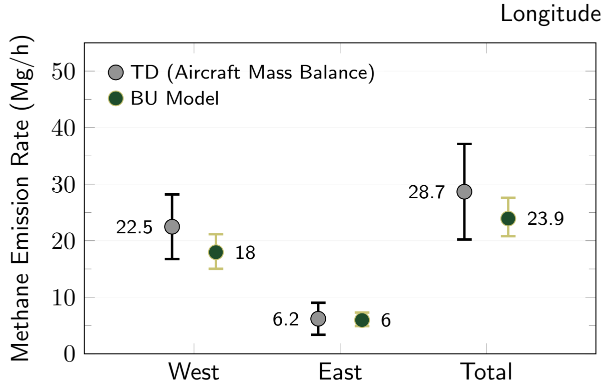

Active Count	West	East
Manual Unloadings	27	5

Figure S1: Bottom-up model results developed using hourly activity data corresponding to the time window of TD aircraft measurements on October 1st.

S1.2 BU Results Summary October 2nd Flight Window

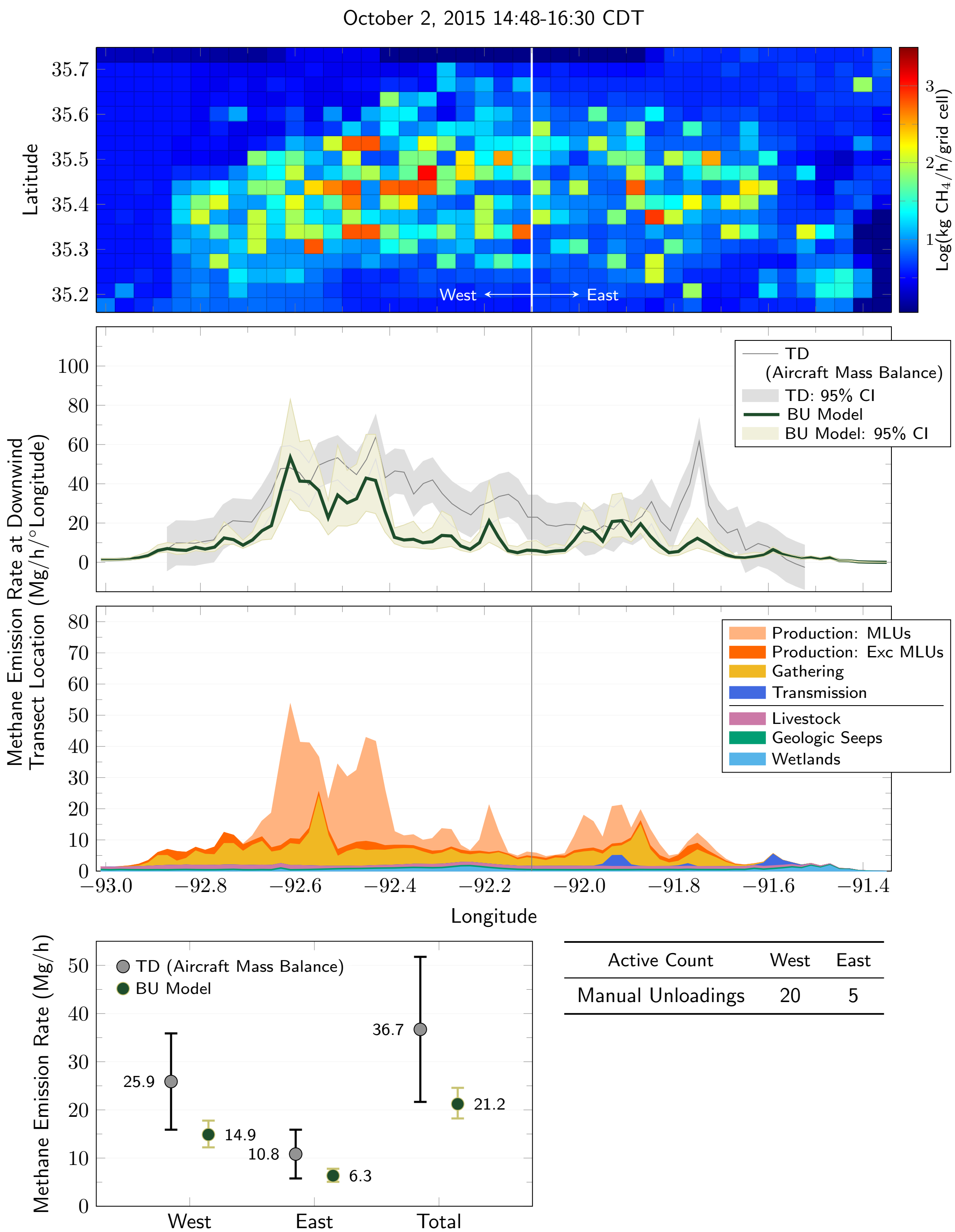

Active Count	West	East
Manual Unloadings	20	5

Figure S2: Bottom-up model results developed using hourly activity data corresponding to the time window of TD aircraft measurements on October 2nd.

S1.3 Supporting Video: Hourly BU Results Animation

Hourly BU model results are summarized graphically for each hour of the 48-hour study period spanning October 1st and 2nd, 2015 in the Supporting Video. An example frame from this animation corresponding to the first hour of the TD flight window on October 1st is shown in Figure S3. Hourly-averaged methane emission rates for the study area estimated by the BU model are shown in the left most panel (a), for production, gathering, transmission, livestock, geologic seeps, and wetlands. Natural gas distribution, rice cultivation, landfills, wastewater treatment, and other source categories contributing less than 1% each to the hourly average are omitted for clarity. The spatial distribution of emissions, simulated BU longitudinal emission rate profiles, aggregate BU emissions for the western, eastern and total study area, and the count of active manual liquid unloadings in the western and eastern portions of the study area are shown (from top to bottom) in panel (b).

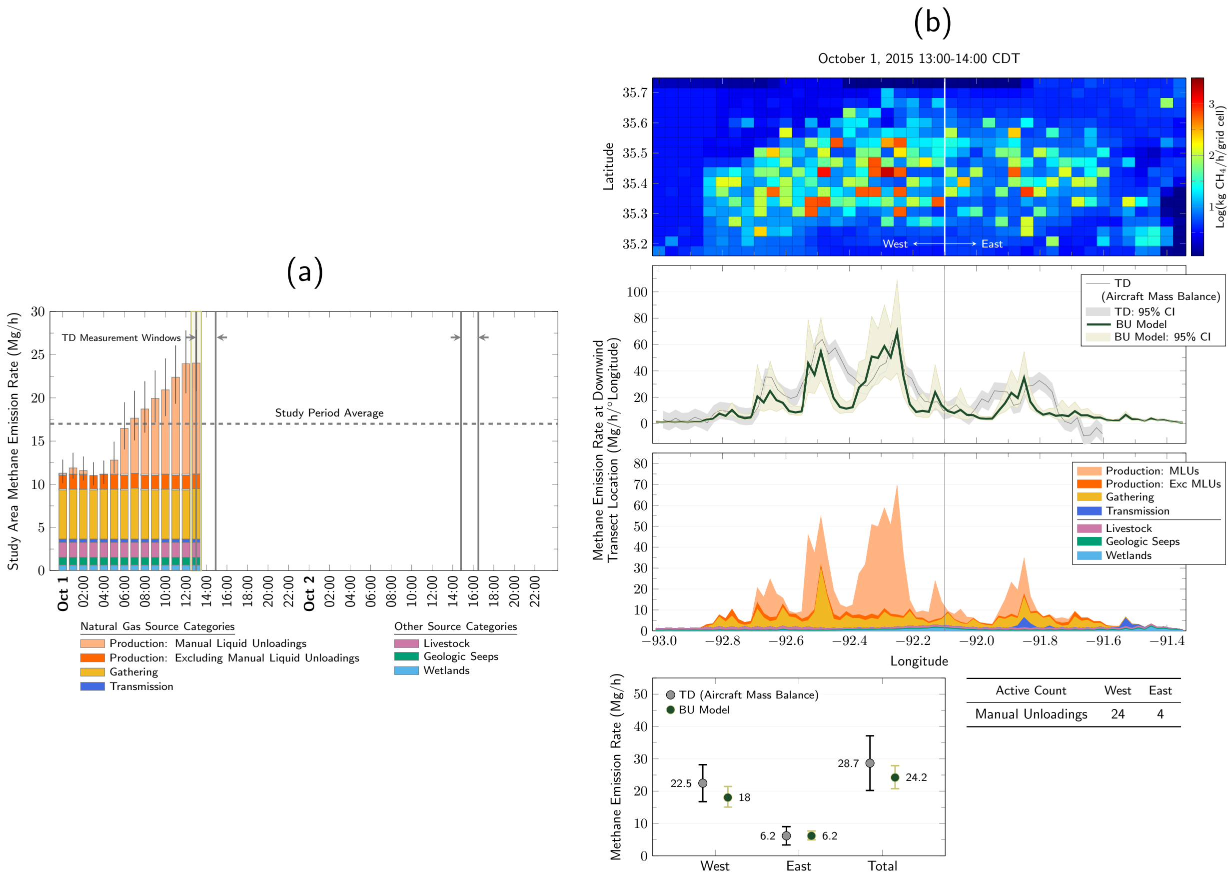

Figure S3: Example frame from the Supporting Video, an animation of hourly BU results spanning the study period.

S2 Hypothetical Emissions Scenario: Estimated Potential Sources

To better understand remaining differences in TD–BU estimates, a hypothetical BU emission scenario was developed that better matched the TD estimate during the first transect of the study area on October 1st. The hypothetical scenario incorporates plausible short-term emission events that represent sub-hourly temporal variations in modeled emissions that may have been captured during aircraft measurements, but were not captured in hourly BU estimates. Nine "estimated potential sources" were added to the BU model with instantaneous emission rates of 600 kg/h, 600 kg/h, 1300 kg/h, 1100 kg/h, 1000 kg/h, 300 kg/h, 500 kg/h, 600 kg/h, and 600 kg/h, from West to East. Each estimated potential source was added at the location of a production or gathering facility capable of producing the instantaneous emission rate modeled, as shown in the top panel of Figure S4. Each source could be thought to represent: a time varying emission source that was observed by the aircraft during a period when the instantaneous emission rate exceeded the average hourly result in the BU model, or a source displaced in time or missing in BU activity data. For example, emission rates from manual liquid unloadings can vary at sub-hourly timescales[1], and blowdowns, compressor engine starts, or other venting activities may not have been accurately logged. The addition of these sources improved the match of aggregate TD—BU estimates (West, East, Total) over the base BU model, and produced a longitudinal emission rate profile whose 95% CI overlapped with TD for 89% of the East—West distance modeled.

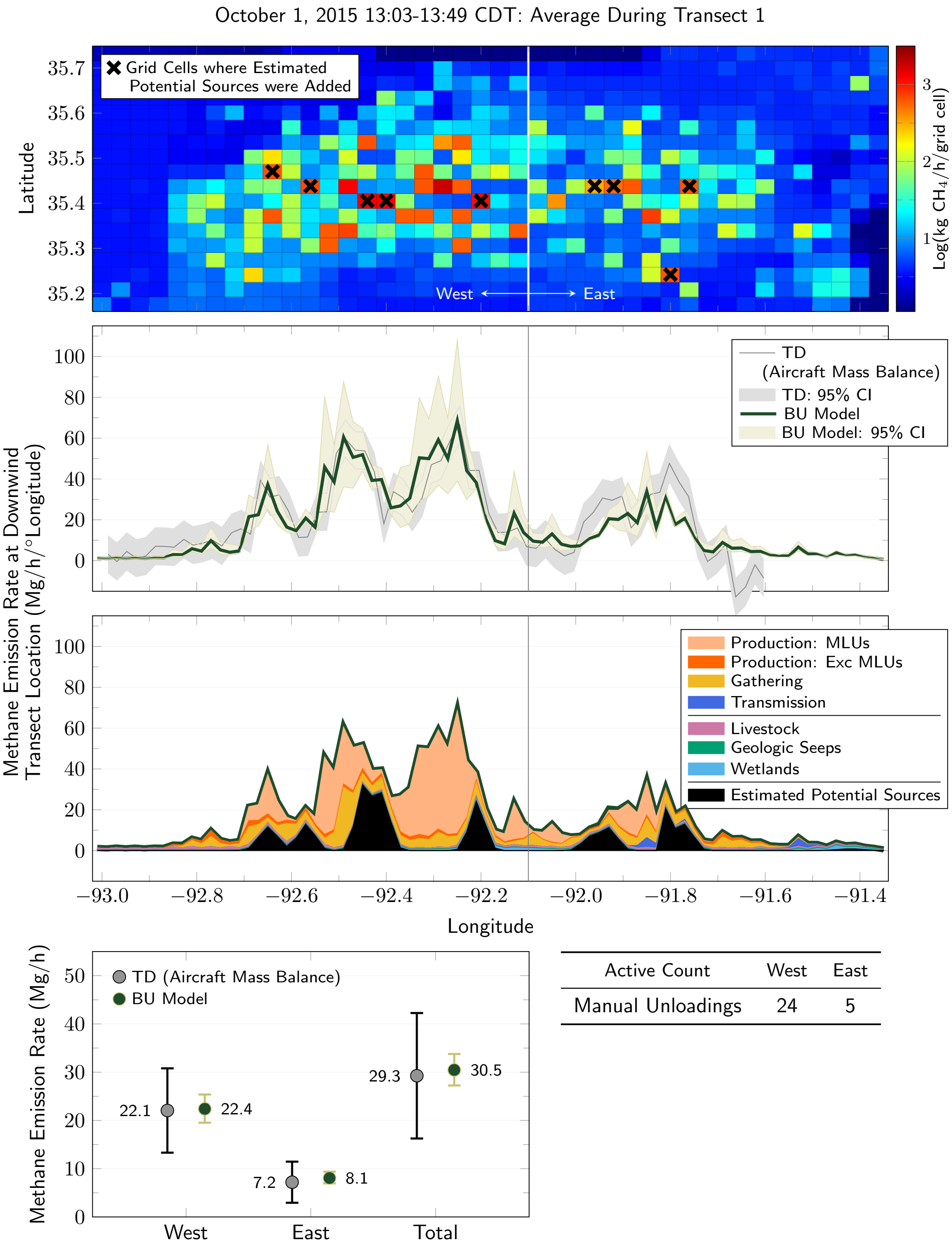

Active Count	West	East
Manual Unloadings	24	5

Figure S4: BU model results during the first TD transect on October 1st, including hypothetical *estimated potential sources* (shown in black) added to the BU model to improve matching between TD and BU central estimates.

S3 BU Model Input and Output Dataset Description

S3.1 BU Model Input Dataset Description

In addition to the BU model input data described herein, input data for MLUs at production facilities and compressor engines at gathering stations are included in *BU_Input_Data_Study_Period.zip*, which contains three files. Start times and durations for MLUs are provided in *ProductionManualLiquidUnloadingTiming.txt* along with counts of production facilities (well pads) and counts of individual wells within BU model grid cells. Compressor engine counts with horsepower by engine type are provided in *GatheringCompressorEngineCountByType.txt*, along with counts of gathering facilities within BU model grid cells. A *ReadMe.txt* file included in *BU_Input_Data_Study_Period.zip* describes the data structure in *ProductionManualLiquidUnloadingTiming.txt* and *GatheringCompressorEngineCountByType.txt*.

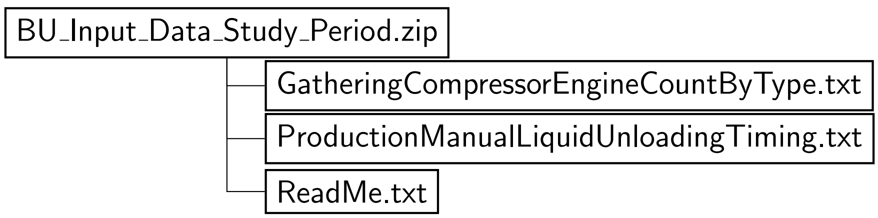

S3.2 BU Model Output Dataset Description

In addition to the graphical results summaries shown in Figures S1 and S2, and the animated study period results (*BU_Summary_Study_Period_SI_Animation.pdf*), results from modeled source categories and sub-categories are provided in tab-delimited format in *BU_Output_Data_Flight_Windows.zip* and *BU_Output_Data_Study_Period.zip*, hereafter the "archives". Each archive includes a *FileListing.txt* with the file tree of the archive. *ReadMe.txt* files in each archive describe the data structure of included files. The archives contain all of the output data computed by the BU model for the mid afternoon flight windows, and the two-day study period spanning October 1st and 2nd respectively.

BU_Output_Data_Flight_Windows.zip contains BU model output averaged over TD flight windows on October 1st and 2nd for all modeled categories. An abbreviated file tree is shown in Figure S5.

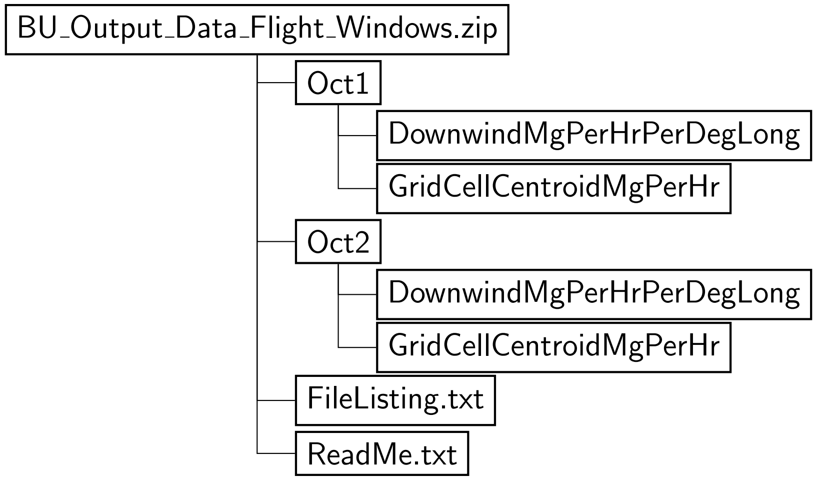

Figure S5

BU_Output_Data_Study_Period.zip contains BU output averaged over each hour-of-day for the 48-hour period spanning October 1st and 2nd for all modeled categories. This archive includes an additional directory, *TimeSeries*, containing three text files with mean and 95% confidence intervals of model outputs for each hour of the 48-hour study period for all modeled categories and sub-categories. This data contains no spatial information and represents aggregate hourly study area emissions by category. An abbreviated file tree is shown in Figure S6.

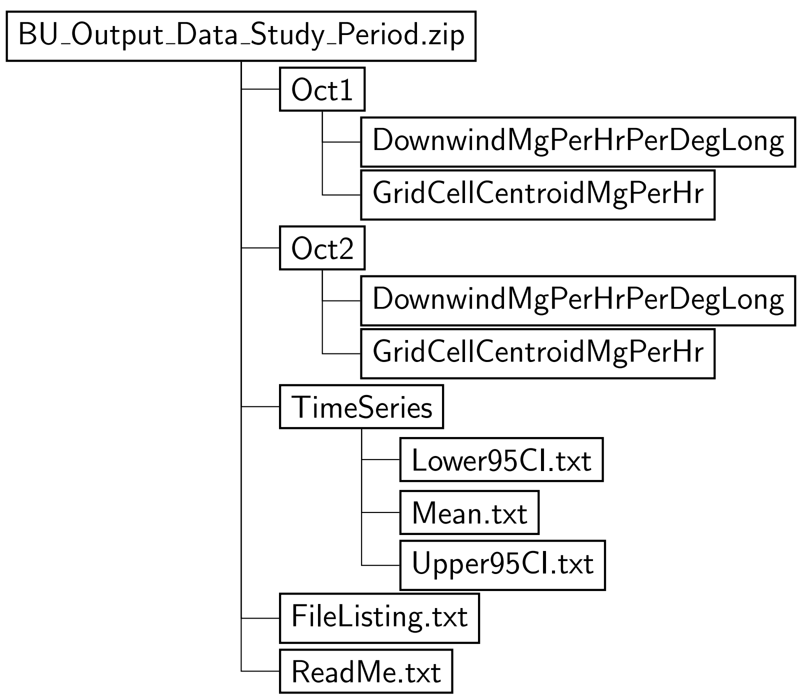

Figure S6

Each of the archives contain directories *Oct1* and *Oct2* which are denoted as *OctX* in the following figures and descriptions. Each *OctX* directory contains directories *Downwind-MgPerHrPerDegLong* and *GridCellCentroidMgPerHr*.

DownwindMgPerHrPerDegLong (see Figure S7) contains directories for each modeled category included in simulated downwind transects. Each directory contains text file(s) with emissions data for the time period modeled. The format of this data is described in the root level *ReadMe.txt*. *StudyAreaTotal* (bold textbox Figure S7) is the sum of all modeled categories shown in normal text boxes. Two subtotals are provided for the production sector: *ProductionSubtotalExcMLU* includes emissions from all modeled production sector categories **except** MLUs. *ProductionSubtotalMLU* includes emissions from manual liquid unloadings only.

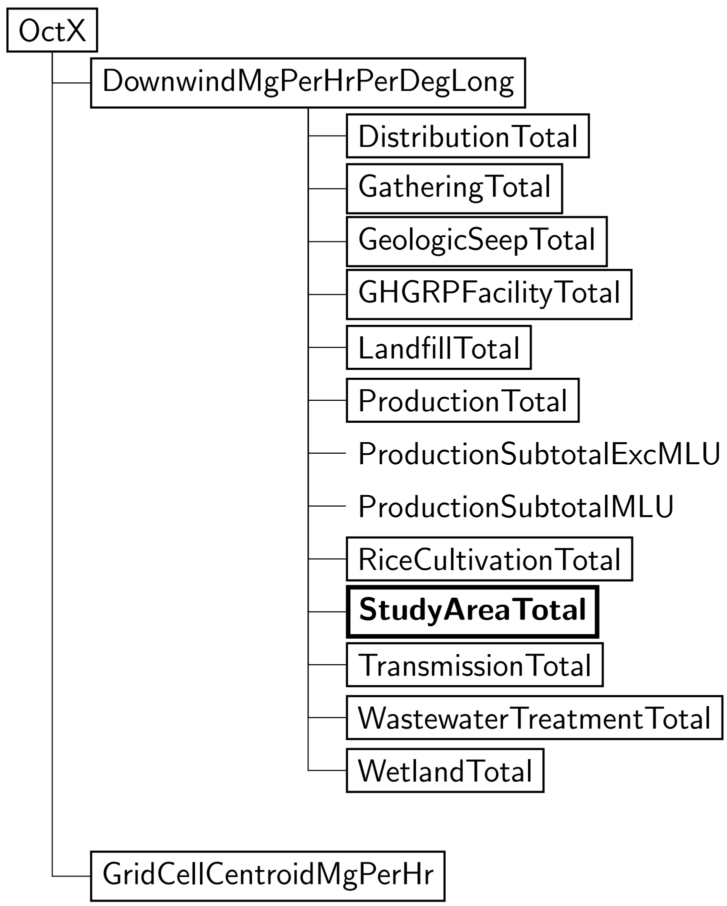

Figure S7: File structure for simulated downwind transect results.

GridCellCentroidMgPerHrPer (see Figure S8) contains directories for each modeled emission category and subcategory. Each directory contains text file(s) with emissions data for the time period modeled which includes the location of the grid cell from which the emissions originated. The location given is the centroid of the BU model grid cell. The format of this data is described in the root level *ReadMe.txt*. *StudyAreaTotal* (bold textbox Figure S8) is the sum of all modeled categories shown in normal text boxes. Each category shown without a textbox is a subtotal of the corresponding category shown in a normal text box. Additional data are provided for the production sector. *ProductionSubtotalExcMLU* includes emissions from all modeled production sector categories **except** MLUs (i.e. *ProductionTotal - ProductionSubtotalMLU*). Counts and durations of MLUs are also included.

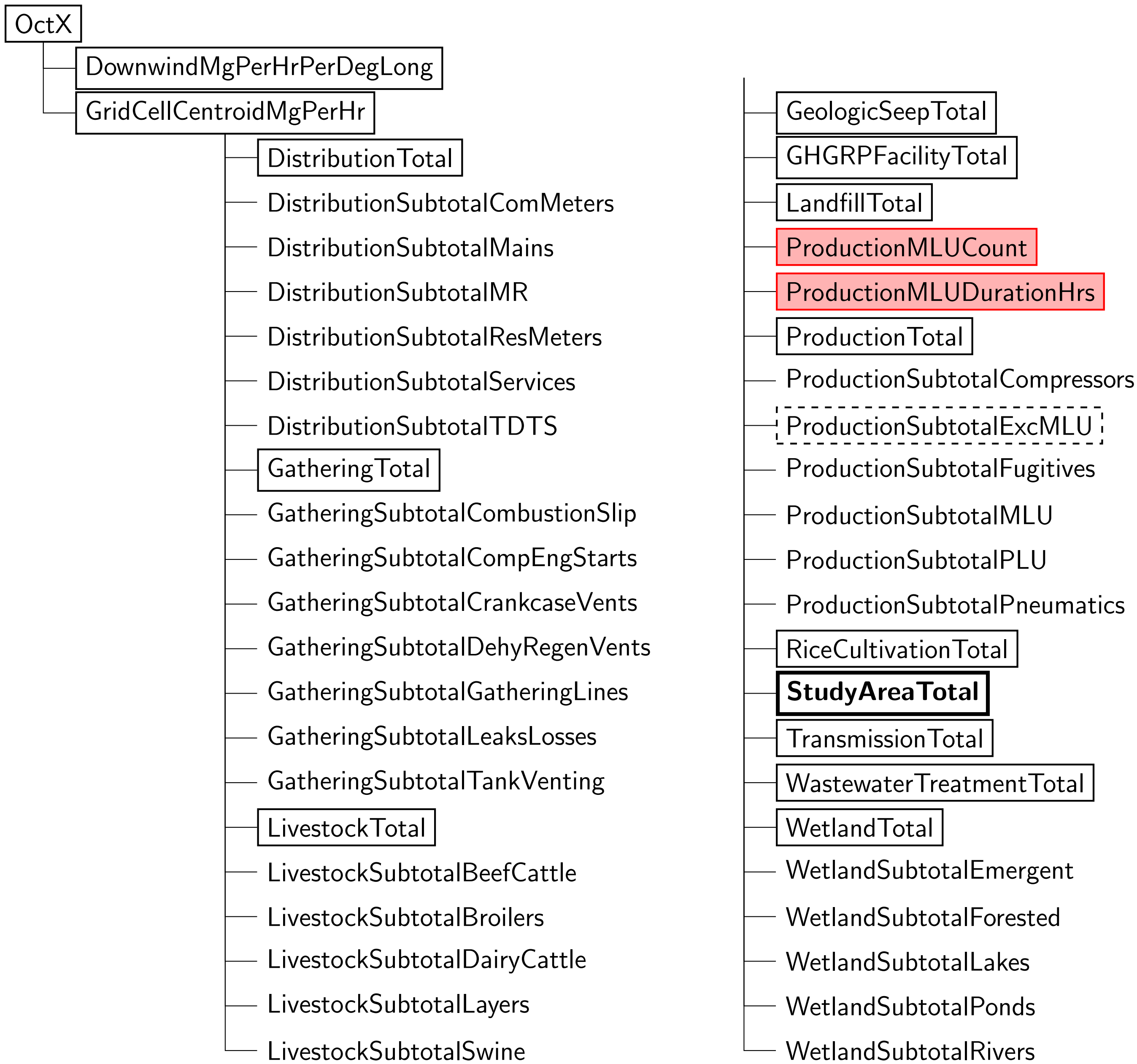

Figure S8: File structure for detailed spatiotemporal BU model results.

S4 BU Model - Study Area Methane Sources

Study area (Figure S9) methane emissions were modeled for O&G operations in the production, gathering, transmission, and distribution sectors. Although some well completion and rework was ongoing, very little drilling activity occurred in the study area during the field campaign; emissions from these sources were not included in the BU model. The well-pad (production) emission rate model, which was developed using detailed activity data and extensive component-level emission measurements made on 261 well pads during the field campaign, is described in Bell et al.[2] Gathering station measurement and modeling methods—which were based upon measurements of 36 compressor stations made during the field campaign using onsite, downwind tracer flux, and facility-scale aircraft measurements—are reported in Vaughn et al.[3] Emissions from distribution systems and gathering pipelines utilize the analysis from Zimmerle et al.[4] Transmission compressor stations were modeled using field campaign measurements[5] and data from EPA's Greenhouse Gas Reporting Program[6].

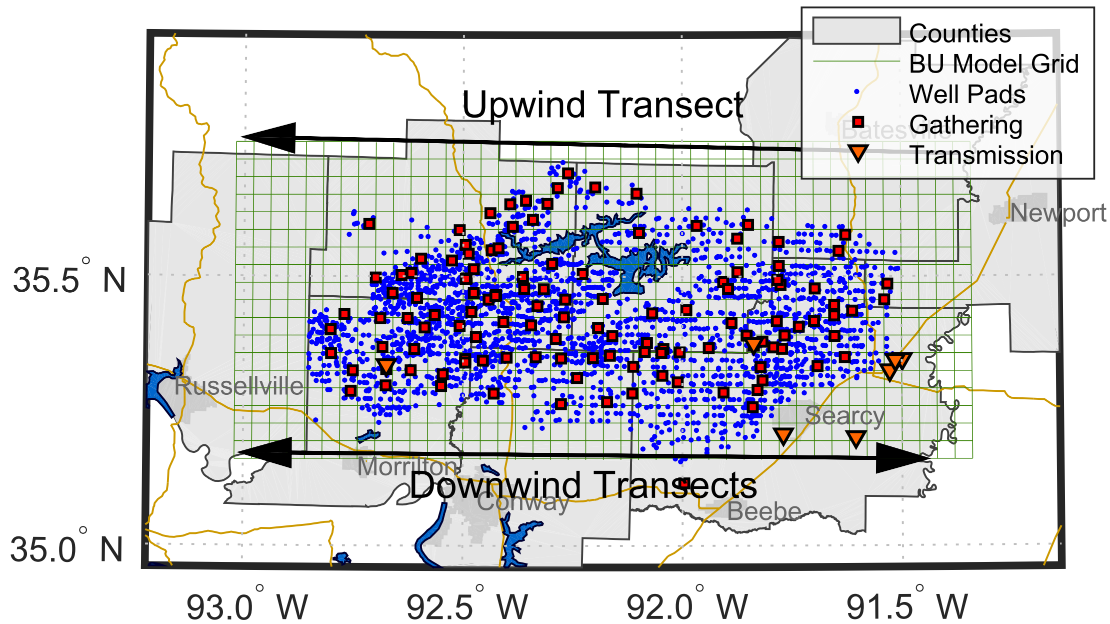

;

Figure S9: Overview of the "study area" in the eastern portion of the Fayetteville shale play in northern Arkansas, USA. Key natural gas infrastructure is shown as blue points for well pads, red squares for gathering compressor stations, and orange triangles for transmission compressor stations. The grid squares utilized in the bottom-up model, shown in green, cover an area approximately 150 km east-west and 65 km north-south at 0.04° (∼3.8 km) resolution. Depicted counties were utilized to compute non-O&G emissions estimates. Approximate location of the aircraft mass balance transects are shown for flights made on October 1st.

Non-O&G emissions sources were generally modeled using the methods described in Schwietzke et al.[7], but spatial resolution was increased herein by calculating methane emissions at the grid cell level where possible. Non-O&G emissions included agricultural operations, lakes and wetlands, naturally-occurring natural gas seepage, and other sources listed in Table S1. Briefly, these sources were estimated using spatially-resolved activity estimates for each source and emission factors from inventories or published sources. These sources represent 20% of the methane emissions during the two-day study period, with approximately 5% from naturally occurring natural gas seepage and approximately 15% from remaining non-O&G sources shown in Table S1. Potential diurnal variations were not estimated for these sources and are not expected to significantly alter the results found in this study.

Table S1: Source categories that contribute to modeled CH_4 emission rates predicted by the BU model.

BU Model Categories	
Oil and Gas	**Non-Oil and Gas**
Production	Livestock
Gathering	Geologic Seeps
Transmission	Wetlands
Distribution	GHGRP Facilities
	Landfills
	Rice Cultivation
	Wastewater Treatment

S4.1 Production

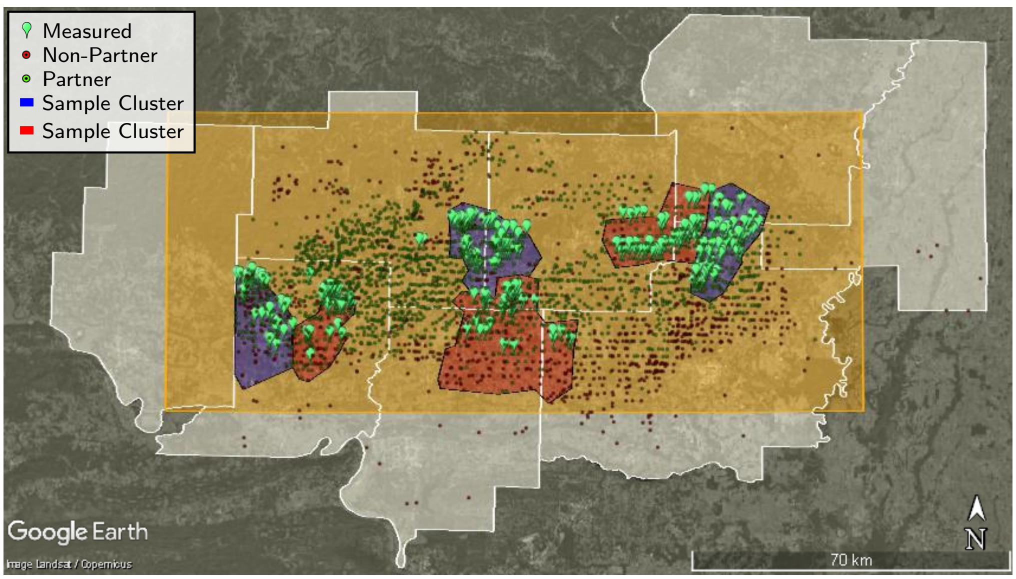

Figure S10: Modeled production sector emissions were based on the study on-site estimate (SOE) of Bell et al.[2]. Study area production facilities (well pads) were chosen for measurement using random sampling, in a clustered sampling strategy.

Emissions from the production sector were modeled based on the study on-site estimate (SOE) of Bell et al.[2], a comprehensive facility-level emission rate estimate. Modeled emissions were categorized as shown in Table S2. The BU model utilized herein modified the calculation of manual liquid unloadings described in Bell et al. to account for transport delay from the location of the unloading to the aircraft downwind transect location.

Manual Unloadings include emissions from vented manual liquid unloadings (MLUs) initiated by workers as a part of normal operations within the study area. MLUs were modeled based on study partner provided activity data and emission rates from a study of liquid unloadings at U.S. natural gas production facilities by Allen et al.[1] Study partners provided spatially and temporally explicit activity data for unloadings at individual wells, including the start times and durations of unloading events. The BU model utilized emission rates for manual liquid unloadings from measurements of horizontal wells without oil production classified as mid-continent in Allen et al.

Emissions from most production source categories exhibit little diurnal variation when aggregated to the basin level. However, emissions from MLUs are typically initiated and terminated by operators during day-time working hours and therefore exhibit substantial diurnal variation. Emissions from MLUs are also the largest emission source in the production sector in the Fayetteville Shale (other basins may differ), and gas quantities released during MLUs are large enough to have a discernable impact on basin-level emissions. "Liquid unloading" refers to the variety of techniques used to remove accumulated liquids from the wellbore that impede the gas flow to the wellhead. Unloading techniques may be manually or automatically initiated, and may lift liquids from the wellbore using rapid gas flow, mechanical devices such as plungers, or chemical "foamers" that enable greater liquid entrainment within the gas stream.[1,8] For this study, we consider only liquid unloadings that vent to atmosphere and are thus directly responsible for methane emissions. For vented MLUs in our study area, an operator typically "shuts in" the well to stop production and allow pressure to build downhole, then opens the well and diverts the flow to produced water tanks at atmospheric pressure. Reduced back pressure from venting gas directly to atmosphere increases gas velocity in the wellbore, aiding in liquid removal. When the wellbore is cleared of liquids, flow is restored to on-site liquid separators and sales pipelines. This procedure may also be used periodically to remove liquids from wells employing other lift methods (e.g., plunger or gas lift).

Plunger Unloadings include emissions from vented plunger unloadings, which may be triggered automatically or manually. Emissions from plunger unloadings were modeled using study partner provided activity data which included annual counts, and average plunger unloading durations. These activity data were spatially explicit and specific to individual wells. The BU model utilized emission rates for mid-continent plunger unloadings measured in Allen et al.[1]

Fugitives as used in herein for the production sector, refers to the sum of Onsite Direct Measurements and Observed/Unmeasured sources as described in Bell et al.[2]

Pneumatics include emissions from pneumatic devices present at production facilities based on study partner provided, spatially explicit counts of pneumatic devices by type, per well. This category includes emissions from: pneumatic-powered chemical injection pumps; continuous high-bleed, continuous low-bleed, and intermittent-bleed pneumatic controllers. Emission rates were simulated based measurement data from Allen et al.[9] for pneumatics in operation in the mid-continent region.

Compressors include combustion slip CH_4 emissions from compressor engines located at production facilities. Other compressor-related emissions were included in *Pneumatics*, or *Fugitives*, as applicable.

Table S2: Production sector source categories that contribute to modeled CH_4 emission rates predicted by the BU model.

Production Model Categories
Manual Unloadings
Plunger Unloadings
Fugitives
Pneumatics
Compressors

S4.2 Gathering

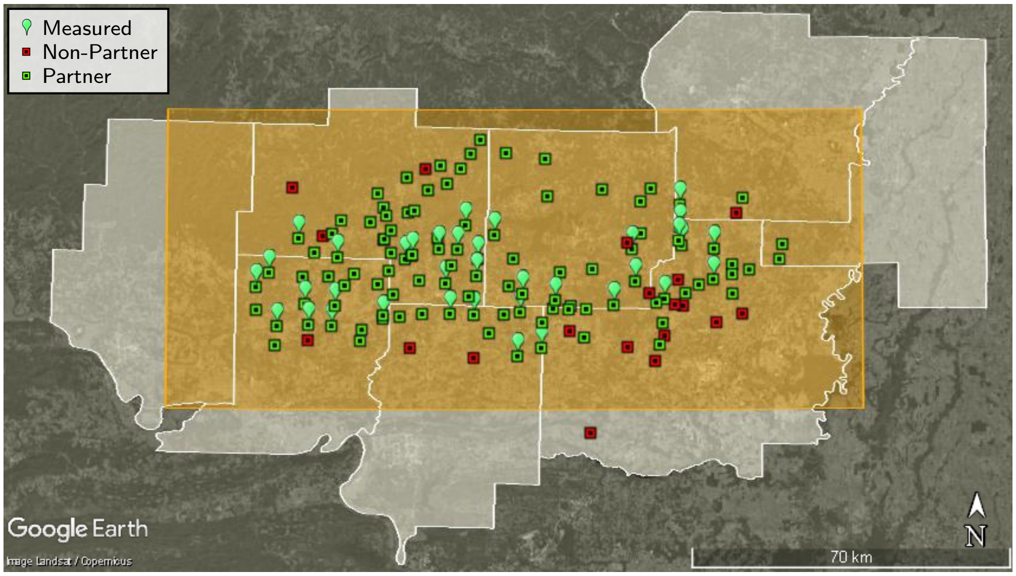

Figure S11: Modeled gathering sector emissions were based on the study on-site estimate (SOE) of Vaughn et al.[3]. Study area gathering stations were chosen for measurement at random from facilities with suitable downwind road access for tracer flux measurements. Nearly all suitable facilities were measured.

Study partners own or manage 99 of the 125 (∼80%) gathering stations located within the study area and provided detailed activity data including facility locations, major equipment inventories, and operating logs. Activity data for non-partner gathering stations were obtained from Arkansas Department of Environmental Quality (ADEQ) permit records; facility locations and compressor engine counts were confirmed using Google Earth. Methane emissions from gathering stations were estimated using on-site measurements, tracer measurements, aircraft measurements, and engineering estimates in a Monte Carlo model based on the SOE model described in Vaughn et al.[3] The SOE was extended to calculate emissions from unmeasured facilities, and a sub-model was added to capture emissions from abnormal process conditions. Abnormal process conditions were modeled based on tracer and aircraft measurements of atypical operating conditions (intended or unintended) made during this study. Emissions were calculated for source categories shown in Table S3 using the methods described in the following sections.

Component or Device Leaks and Losses (hereafter "leaks") refer to on-site direct measurements (ODMs) and simulated direct measurements (SDMs) of sources as described in Vaughn et al.[3] ODMs refer to measurements made by on-site teams during the field campaign using high-flow samplers (Bacharach Hi Flow®). ODMs were made of dry gas sources spanning the measurable range of the high-flow sampler (0.05 SCFM–8 SCFM or equivalently 0.058–9.24 kg/h).[10] SDMs provide an emission rate estimate when ODMs were attempted but outside the measurable leak rate of the high-flow sampler, or when sources were observed with optical gas imaging (OGI) but were not safe or accessible for measurement. Simulated direct measurements were re-sampled from ODMs of the same major equipment category. Measured and unmeasured leaks observed with OGI and estimated to be within the measurable range of the high-flow sampler are termed

Table S3: Gathering sector source categories that contribute to modeled CH_4 emission rates predicted by the BU model.

Gathering Model Categories
Component or Device Leaks and Losses
Combustion Slip
Crankcase Vents
Dehydrator Regenerator Vents
Compressor Engine Start-ups
Tank Venting
Gathering Lines

"leak observations".

Table S4: All on-site direct measurements made at gathering stations during the field campaign were assigned to one of the following categories.

Gathering Major Equipment Categories
Compressor
Dehydrator
Other
Pig Launcher/Receiver
Piping or Gas Line
Separator
Tank

At measured gathering stations CH_4 emissions from leaks were calculated as described in Vaughn et al.[3] To estimate leaks at un-measured gathering stations, leak count distributions were developed by dividing leak observation counts by major equipment counts at each measured facility. For example, all leak observations on dehydrators (excluding regenerator vents) at a measured facility were divided by the number of dehydrators at the facility, resulting in a distribution of dehydrator leaks per dehydrator. Leak observations from all other major equipment categories were normalized similarly using compressor engine counts. Compressor leaks were further disaggregated to distinguish rod packing vent and pressure relief valve emissions from other leaks.

For each Monte Carlo iteration, i, methane emissions from leaks at un-measured facility j were calculated in a two-step process. First, the number of leak observations was simulated for each major equipment category as:

$$N_{leakobs,i} = \sum_{k=1}^{N} \text{round}(\text{draw}(\text{Dist}) \cdot N) \tag{1}$$

Where:

N is the count of major equipment category k at facility j (compressors or dehydrators) draw(Dist) indicates drawing one value at random from the distribution of normalized leak observations for major equipment category k

The result is a simulated leak observation count for each major equipment category at an unmeasured facility. The CH_4 emission rate from leaks in major equipment category k is then simulated based on the leak observation count as:

$$\dot{m}_{leaks,i} = \sum_{k=1}^{N_{leakobs}} \text{simulate}(leakobs_k) \tag{2}$$

Where:

$N_{leakobs}$ is the count of leak observations simulated for major equipment category k in equation 1

simulate($leakobs_k$) indicates simulating a leak observation as described in Vaughn et al.[3]

Combustion Slip refers to unburned fuel entrained compressor engine exhaust. Combustion slip was not measured in this study; however, study partners provided engine exhaust stack test data for 111 engines located within the study area tested in the year prior to the field campaign. Tests were performed by measurement contractors using standard methods (EPA Method 19[11], EPA Method 320[12]). Of the 111 engines tested, 24 were from one engine series (Caterpillar® G3500, rated at ≈1 MW), and 87 from another (Caterpillar® G3600, rated at ≈1.3 MW). Activity data from study partners and ADEQ indicate that the study area contains 447 gathering compressor engines, 416 of which belong to one of these two engine series. These tests therefore represent nearly one fourth of the compressor engines at gathering stations within the study area and nearly all (93%) compressor engines belong to one of these engine series, leading to high confidence in combustion slip estimates. All engines belonging to the two series tested were simulated using emission factors developed from test data. The 31 gathering compressor engines within the study area that did not belong to one of these engine series were simulated using Environmental Protection Agency (EPA) AP-42[13] factors relevant to the engine classification.

Study partners also provided activity data for compressor engines that included run-hours, start-up times, and shut-down times for approximately 70% of gathering compressor engines within the study area. Combustion slip emissions were calculated for each hour of the study period using this activity data. Run hours and start-ups and shut-downs were applied directly to the engines they were provided for; all other engines were simulated by re-sampling from this data.

For each Monte Carlo iteration, i, combustion slip methane emissions for facility j were calculated as:

$$\dot{m}_{combslip,i} = \sum_{k=1}^{N_{op}} EF_k \cdot \text{draw}(Load_k) \cdot RatedHP_k \tag{3}$$

Where:

N_{op} represents the count of compressor engines operating on-site for the hour simulated, whether known explicitly or simulated by re-sampling

EF_k is the emission factor relevant to engine k. EF_k is re-sampled from study partner provided test data for Caterpillar® G3500, and G3600 series engines. AP-42 factors were used otherwise.

draw($Load_k$) indicates drawing a fractional load at random from the distribution of operating loads observed during the field campaign, and applying it to engine k

$RatedHP_k$ is the rated power output of engine k

Crankcase Vents account for CH_4 vented from compressor engine crankcases because of imperfect piston ring sealing. Crankcase vents were simulated based on a Caterpillar® crankcase ventilation system application guide[14]; crankcase vents were not measured in this study. Expected crankcase vent hydrocarbon emissions are normally 3% of exhaust hydrocarbon emissions at engine mid-life, but could reach 20% due to engine wear. Crankcase vent emissions were simulated by multiplying combustion slip by a factor drawn at random from a normal distribution (mean 3%, assumed standard deviation 2%).

Dehydrator Regenerator Vents were simulated using the emission factor for dehydrators with flash tank vapor recovery from a 1996 GRI study[15] (0.003 (-52%/+102%) kg/h CH_4 per MMscf per day of gas processed). Most study partner dehydrators were equipped with flash tank vapor recovery, an emission control technique. The volume of gas processed is directly related to operating compressor engine horsepower, and was estimated on this basis.

For each Monte Carlo iteration, i, methane emissions from measured glycol dehydrator still vents at facility j were calculated as:

$$\dot{m}_{measdehy,i} = \begin{cases} \sum_{k=1}^{N} f_i \cdot ODM_{stillvent,k} & \text{if measured,} \\ 0 & \text{otherwise} \end{cases} \tag{4}$$

Where:

N is the number of on-site direct measurements of dehydrator still vents made at facility j not subject to any emission rate exceptions

f_i is a factor drawn from a normal distribution to account for the high-flow sampler measurement uncertainty ($\pm$ 10%)[10]

Compressor Engine Start-ups account for emissions released from gas pneumatic starters and pumps used to start compressor engines. Study partners provided an estimate of 3800 scf of gas released per engine start. Emissions were simulated by drawing a value at random from a triangular distribution centered at 3800 scf, and ranging from 500 scf–5000 scf. Engine start-up times and locations were known for 70% of study area engines, and were simulated otherwise.

Tank Venting refers to abnormal process conditions that resulted in continuous emissions from tanks well in excess of the measurable leak rate of the high-flow sampler. This scenario was encountered on two occasions during the field campaign and both were simulated in the BU model. In one instance, the aircraft team noted significant CH_4 enhancement from a gathering station during a raster flight. The facility was measured[16] on three days (October 2st,3rd, and 14th, 2015) with emission rates of 276 ($\pm$ 99 kg/h), 676 ($\pm$ 119 kg/h), and 739 ($\pm$ 107 kg/h) on each day, respectively. Tracer and on-site measurements were made at this facility on October 6th, 2015. The source was identified as a produced water tank and the cause was identified as an open (hand-operated) valve on a compressor engine fuel scrubber. The tracer team was not able to make a complete facility measurement, but was able to measure the portion of the facility where the tank was located both with the valve open, and after it had been identified and closed. Subtracting the tracer estimates made in each operating state leads to an estimated 606 ($\pm$ 278 kg/h) originating from the tank. On-site teams had no means to quantify or estimate an emission source of this magnitude.

For this facility only, on each Monte Carlo iteration, i, tank venting emissions were calculated by first randomly choosing a measurement day. If an aircraft measurement date is chosen, the emission rate for all other sources at the facility (as predicted by the SOE) is subtracted from the aircraft measurement and uncertainties were subtracted in quadrature. A random value is then selected from a triangular distribution centered at the difference, and bounded by the uncertainty (95% CI). If the tracer measurement date is chosen, a random value is selected from a triangular distribution described by the tracer measurement and associated uncertainty (95% CI). Tank emissions at this facility are a self-representing sample since the facility was not chosen for measurement randomly. Ground-based teams were dispatched to confirm the aircraft measurements. The aircraft did not identify any other facilities with persistent emission rates of this magnitude during the field campaign.

In another instance, tank venting was observed at a gathering station during random sampling. At this facility, the tracer team noticed significant CH_4 enhancement from a produced water tank, which on-site measurement teams confirmed as the source via OGI. The cause was not identified, but operators at the facility suspected a stuck dump valve. Tank venting emissions were estimated by subtracting the SOE from the tracer measurement at this facility, since the SOE estimates all sources except the tank venting, and the tracer measurement captures all sources including the tank venting. The estimated tank venting emission rate was 140 ($\pm$ 40 kg/h). The tracer team did not identify similar tank venting emissions at other measured gathering stations. We assume that the emission rate and observed frequency are representative of tank venting emissions from gathering stations within the study area. Each simulated gathering station (except the self-representing facility described previously) was assigned tank venting emissions at the probability observed, approximately 1 in 30. If a gathering facility was assigned tank venting emissions, an emission rate was drawn at random from a triangular distribution described by the estimated emission rate and associated uncertainty.

Gathering Pipelines herein refer to both underground pipelines and associated above ground equipment, and were simulated as described in Zimmerle et al.[4]. During the field campaign, 96 kilometers of gathering pipelines and associated above ground equipment were surveyed and measured, including 56 pigging facilities and 39 block valves. Only one underground pipeline leak was identified and it accounted for 83% (4 kg/h) of measured emissions from gathering pipelines. Leaks were found most often on above-ground equipment. Zimmerle et al. estimate total study area CH_4 emissions from gathering pipelines of 400 kg/h (+214%/-87%, 95% CI).

For each Monte Carlo iteration, total methane emissions from gathering pipelines in the study area were calculated using the method described in Zimmerle et al.[4] Total emissions were then distributed to grid cells using a correlation based on the spatial density of wells. CH_4 emissions from gathering stations and gathering lines were assigned to the grid cells containing them.

S4.3 Transmission

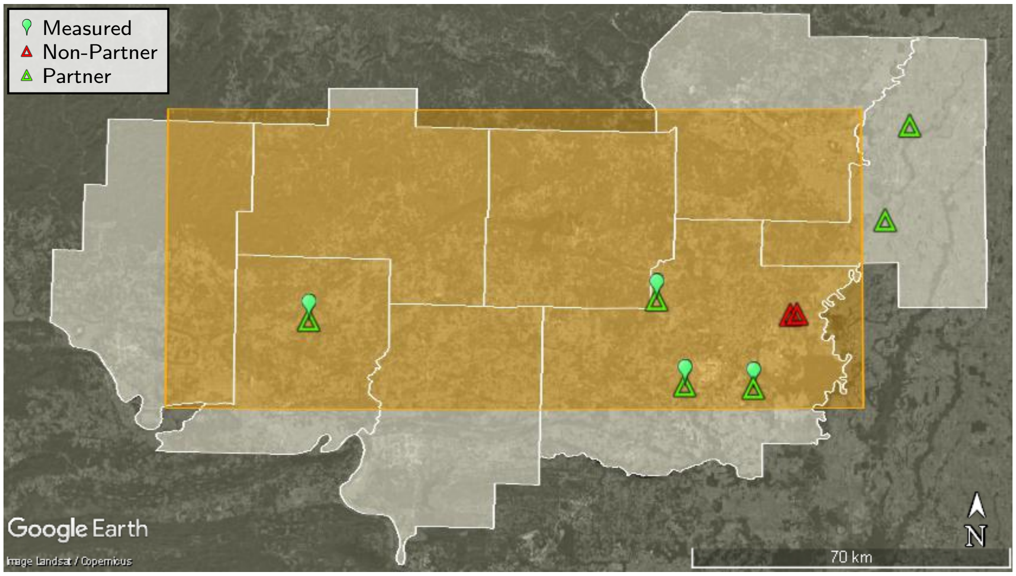

Figure S12: Study partners operated four of the six transmission stations located in the study area. Emissions from these four stations were modeled based on tracer measurements made during this study. Emissions from the two non-partner transmission stations were modeled based on EPA GHGRP data.

Four study partner transmission stations and two non-partner transmission stations were identified within the study area using study partner data, GHGRP data, and ADEQ records. Methane emissions from study partner transmission stations were estimated using tracer measurements made during this study. Emissions from non-partner transmission stations were calculated from data reported to the EPA GHGRP. First, CH_4 emissions for stationary combustion reported under 40 CFR 98.33.[17] ("Subpart C") were recalculated using AP-42[13] emission factors. These results were then added to emissions reported under 40 CFR 98.230[18] ("Subpart W") and normalized to provide an annual average hourly emission rate for the non-partner facilities. On-site measurements were not made at transmission stations in this study. A 95% confidence interval of $\pm$50% is assumed for these emission rates.

For each Monte Carlo iteration, i, CH_4 emissions from transmission stations were calculated as follows:

$$\dot{m}_{trans,i} = \sum_{m=1}^{4} \text{draw}(\dot{m}_{meas,m}) + \sum_{r=1}^{2} \text{draw}(\dot{m}_{ghgrp,r}) \quad (5)$$

Where:

draw($\dot{m}_{meas,m}$) indicates drawing one emission rate at random from a normal distribution described by tracer measurement and associated uncertainty at each of four measured facilities

draw($\dot{m}_{ghgrp,r}$) indicates drawing one emission rate at random from a triangular distribution centered at the calculated annual average hourly emission rate, with assumed 95% CI of $\pm$50%

Calculated emissions were assigned spatially to the transmission category in the grid cells that contain the facilities.

S4.4 Distribution

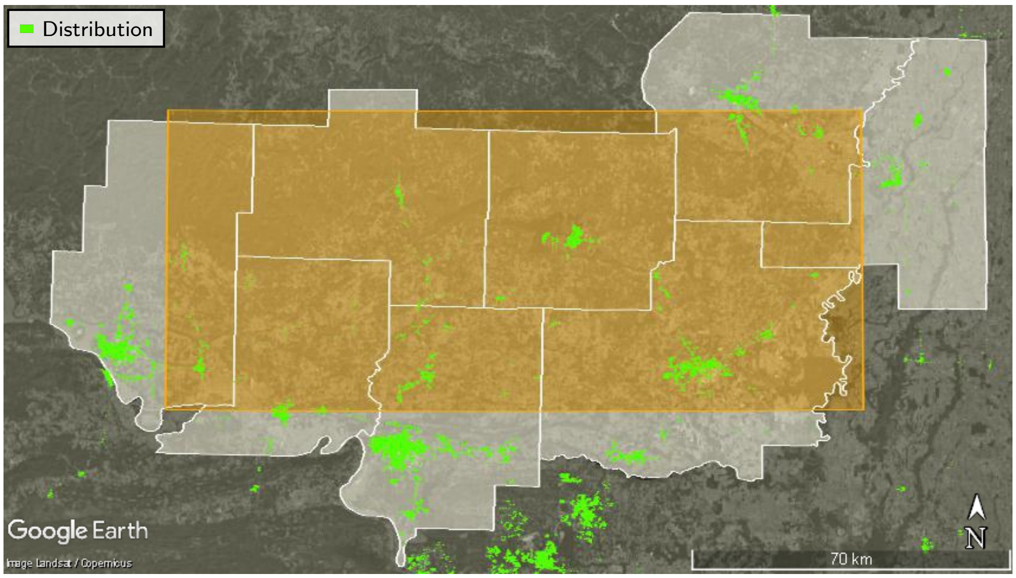

Figure S13: Distribution sector activities are concentrated in urban and suburban regions. One study partner distribution company serves the entire study area.

Methane emissions from the distribution sector were estimated based on direct measurements performed during this study and activity data provided by study partners for most source categories. Sources with few or no measurements were estimated using activity data and emission factors from this and prior studies. One distribution company serves the entire study area, enabling measurement across the entire industry sector. Distribution operations are concentrated mainly in urban and suburban areas with higher population density, as highlighted in Figure S13.

Leaks were measured at distribution facilities and on distribution pipelines. Distribution facilities were classified as transmission distribution transfer stations (TDTSs), metering and regulating (M&R) stations, or customer meters, while pipelines were classified as service mains, or service pipelines. Gas from transmission pipelines enters the TDTS on the "transmission side" and the pressure is reduced (from ∼1,000 psi to ∼100–500 psi) as the gas flows to the "distribution side" and enters the distribution system. A TDTS may contain equipment owned and operated by both the transmission and distribution operators, for example both operators typically measure gas flow during the custody exchange. Gas exiting the TDTS is routed to service mains which deliver it to M&R stations, where the gas flow is measured ("metering") and pressure is further reduced. Metering was not performed at M&R stations within the study area because the system was wholly owned by a single operator. Gas exiting M&R stations is routed to service pipelines that deliver it to customer meters at commercial or residential locations.

Measured TDTS and M&R stations were grouped into three categories based on the gas pressure at the inlet to the facility. At some TDTSs the transmission side of the facility was not measured because study personnel did not have right-of-access at the start of the field campaign.

Table S5: Distribution sector source categories that contribute to modeled CH_4 emission rates predicted by the BU model.

Distribution Model Categories
Transmission Distribution Transfer Stations
Service Main Pipelines
Service Pipelines
Metering and Regulating
Commercial Sales Meters
Residential Sales Meters

Therefore, the transmission and distribution sides of TDTSs were modeled independently to ensure inclusion of potential emissions at stations where the transmission side was not measured. Leak surveys were not performed to identify pipeline leaks. Pipeline leaks targeted for measurement were selected at random from a list of reported or identified leaks maintained by the partner company. This list was assumed to contain all distribution pipeline leaks within the study area that may have existed during the study period. A detailed description of the distribution measurements made during this study were provided by Pickering.[19]. Only a small number of sales meters included in the reported leak list were measured during the study. Emission estimates for sales meters were therefore based on measurements made in this study, and a prior study which measured a large number of commercial and residential sales meters.[20]

Table S6: Counts of measurements made at distribution facilities during the field campaign.

County	M&R[a]	Pipelines[b] Mains	Pipelines[b] Services	TDTS[a] Distributionn Side	TDTS[a] Transmission Side
Cleburne	5/5	0/1	0/0	6/6	6/6
Conway	10/10	0/0	0/0	7/8	6/8
Faulkner	30/37	2/3	5/11	9/11	9/11
Independence	0/47	0/5	0/6	0/3	0/3
Jackson	0/27	0/5	0/1	0/2	0/2
Pope	15/15	1/4	5/9	4/5	4/5
Van Buren	27/27	0/0	0/0	1/1	0/1
White	13/29	11/23	10/17	2/6	0/6

[a] Measured facilities / total facilities
[b] Measured leaks / reported or otherwise identified leaks

For each Monte Carlo iteration, i, CH_4 emissions from distribution facility category k in county j were calculated as follows:

$$\dot{m}_{category(k),i} = (\text{draw}(EF_k) \cdot AD_k + MEAS_{category(k)}) \cdot (Area\cap_j) \tag{6}$$

Where:

draw(EF_k) indicates drawing one emission rate at random for facility $category(k)$

AD_k indicates the activity data (facility count) for $category(k)$ for county j

$MEAS_{category(k)}$ is the sum of all measurements for $category(k)$ in in county j

$Area\cap_j$ is the fraction of county j that spatially intersects the study area

Emissions were assumed to be distributed uniformly throughout the regions with distribution service (Figure S13) and were apportioned to grid cells in a two-step process. First, emissions from distribution operations in county j were scaled by the fractional area of distribution operations in county j that spatially intersect the study area. Second, emissions were apportioned to grid cells by the fractional area of distribution operations that spatially intersect an individual grid cell. In this way, county level activity data, and measured and simulated emissions were concentrated in regions with distribution operations, and were scaled by the overlap with the study area. This also allows emissions to be attributed appropriately to grid cells that intersect distribution operations in multiple counties.

S4.5 Livestock

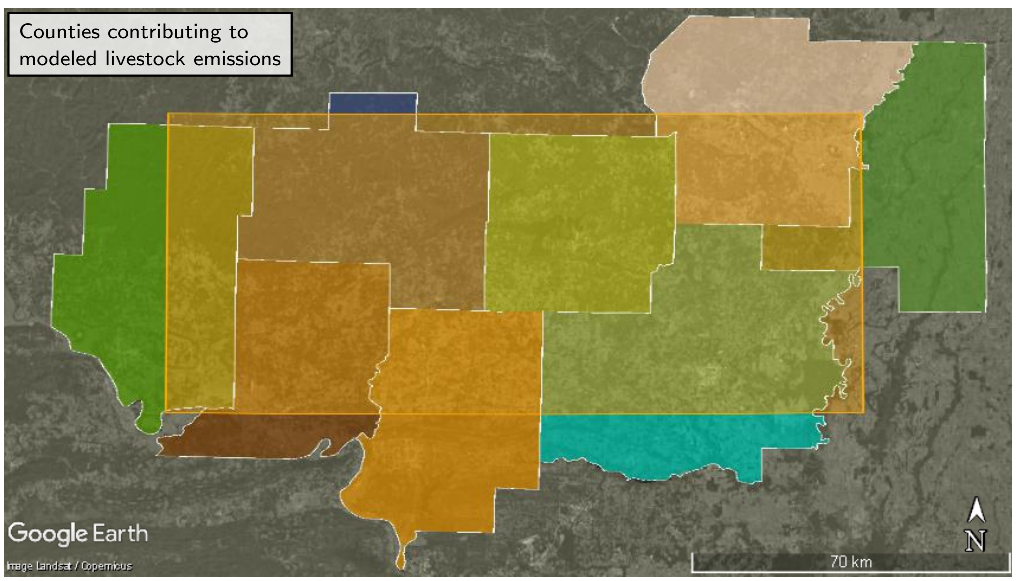

Figure S14: Livestock data were only available at the county-level, and were apportioned to the study area (orange rectangle) in proportion to spatial intersection with the counties shown.

Methane emissions from livestock were calculated using activity data from the United States Department of Agriculture (USDA) census and emission factors from the U.S. EPA greenhouse gas inventory (GHGI)[21], and Intergovernmental Panel on Climate Change (IPCC)[22] guidelines. Livestock counts were obtained at the county level from the 2012 USDA census[23] for the eight Arkansas counties that significantly overlap the study area. Data were not available for all source categories for all counties because data is withheld in cases where it can be attributed to a unique producer. In cases where 2012 data were withheld, 2007 data were used instead. If neither 2012 nor 2007 data were available for a category, its activity data was considered 0 in this model.

Table S7: 2012 USDA livestock census data for study area counties.

USDA County-Level Activity Data

County	Beef Cows	Milk Cows	Other Cattle	Hogs	Layers	Pullets	Broilers
Cleburne	13 606	0	206 706	140	389 627[1]	134 030[1]	1 991 264[1]
Conway	20 303[1]	1130[1]	29 718[1]	12 512	62 928	114	6 888 751
Faulkner	14 390	886	14 892	129	2525	196	76
Independence	19 533	0	16 520	104	367 690	718 857	6 665 939
Jackson	2288	0	2170	0	386	D[2]	D[2]
Pope	16 181	0	13 689	9380	155 763	303 221	4 871 203
Van Buren	11 135[1]	790[1]	8372[1]	3103[1]	1031	164	489 312
White	20 234	401	21 316	408	D[2]	D[2]	806 465

[1] 2007 USDA census data used
[2] Withheld to avoid disclosing data for individual farms

The USDA census inventories cattle as 'beef cows', 'milk cows' and 'other cattle'. Emission factors are available from the GHGI[21] for 'dairy cattle' and 'beef cattle'. For this reason, 'other cows' from the AR USDA county level census data were redistributed proportionally to the 'milk cow' and 'beef cow' categories. The only poultry considered in this model were chicken. Chicken were inventoried in the USDA census as 'layers', 'pullets' and 'broilers'. Pullets grow to be layer flock replacements and were therefore added to the layer inventory in this model. No uncertainty was applied to livestock activity data.

Table S8: 2012 USDA livestock census data for study area counties, as modeled.

Modeled County-Level Activity Data

County	Beef Cows	Milk Cows	Hogs	Layers	Broilers
Cleburne	34 276	0	140	523 657	1 991 264
Conway	48 454	2697	12 512	63 042	6 888 751
Faulkner	28 418	1750	129	2721	76
Independence	36 053	0	104	1 086 547	6 665 939
Jackson	4458	0	0	386	0
Pope	29 870	0	9380	458 984	4 871 203
Van Buren	18 952	1345	3103	1195	489 312
White	41 136	815	408	0	806 465

Emission factors used for livestock categories considered in the model are shown in Table S9. Emission factors are the U.S. implied emission factors developed in the GHGI[21], and uncertainties are 95% confidence intervals provided in the IPCC[22] guidelines for GHGIs.

For each Monte Carlo iteration, i, CH_4 emissions from livestock category k in county j were calculated as follows:

$$\dot{m}_{category(k),i} = \text{draw}(EF_k) \cdot (AD_k) \cdot (Area\cap_j) \tag{7}$$

Where:

draw(EF_k) indicates drawing one emission factor value at random from a triangular distribution centered at EF_k, and bounded by its associated confidence interval, as shown in Table S9

Table S9: Emission factors and uncertainty used in the model for estimating CH_4 emissions from livestock.

Livestock Emission Factors Used In Model

Category	CH_4 Emission Factor (g/head/hr)[a]	95% Confidence Interval[b]
Beef Cattle Enteric Fermentation	8.4	$\pm 50\%$
Beef Cattle Manure Management	0.2	$\pm 30\%$
Dairy Cattle Enteric Fermentation	13.5	$\pm 50\%$
Dairy Cattle Manure Management	8.0	$\pm 30\%$
Swine Enteric Fermentation	0.2	$\pm 50\%$
Swine Manure Management	1.6	$\pm 30\%$
Poultry Manure Management	0.01	$\pm 30\%$

[a] US EPA GHGI[21]
[b] IPCC guidelines[22]

AD_k indicates the activity data (head count) for $category(k)$ for county j

$Area\cap_j$ is the fraction of county j that spatially intersects the study area

Emissions were assumed to be distributed uniformly throughout the county area and were apportioned to grid cells in a two-step process. First, emissions from county j were scaled by the fractional area of county j that spatially intersects the study area, resulting in a sub-county emission estimate. Second, sub-county emissions were apportioned to grid cells by the fractional area of sub-county j that spatially intersects an individual grid cell. In this way, county level emissions were scaled by the area overlap with the study area and emissions were attributed appropriately to grid cells that intersect multiple counties.

S4.6 Rice Cultivation

Methane emissions from rice cultivation were calculated based on a combination of IPCC factors[22] and USDA county level census data for the state of Arkansas.[23] Arkansas has the largest area of rice harvested in all U.S. states.[21] However, the majority of CH_4 emissions from rice cultivation occur during the growing season when fields are flooded. Rice is typically harvested in early September, and was thus likely harvested before the mass balance flights which occurred on October 1st and 2nd. One study of Arkansas rice fields[24] found that post-harvest CH_4 emissions represented 2% of annual emissions. Therefore we have multiplied the IPCC rice emission factor by 0.02 to develop a study relevent CH_4 emission factor for rice cultivation.

For each Monte Carlo iteration, i, CH_4 emissions from rice cultivation in county j were calculated as follows:

$$\dot{m}_{rice,i} = \text{draw}(EF_{rice}) \cdot (AD_{rice}) \cdot (Area\cap_j) \tag{8}$$

Where:

draw(EF_{rice}) indicates drawing one emission factor value at random from a triangular distribution centered at EF_{rice}, and bounded by its associated confidence interval

Table S10: The emission factor for rice cultivation used in the GLAE is based on IPCC guidelines, modified to represent post-harvest CH_4 emissions.

Rice Cultivation Emission Factor Used In Model

Emission Source	CH_4 Emission Factor (kg/hr/m^2)	95% Confidence Interval
Rice Cultivation[a]	108×10^{-9}	$-39\%/+70\%$

[a] IPCC[22] default emissions factor modified by Smartt et al.[24]

AD_{rice} indicates the activity data (area harvested) for county j

$Area\cap_j$ is the fraction of county j that spatially intersects the study area

Emissions were assumed to be distributed uniformly throughout the county area and were apportioned to grid cells in a two-step process. First, emissions from county j were scaled by the fractional area of county j that spatially intersects the study area, resulting in a sub-county emission estimate. Second, sub-county emissions were apportioned to grid cells by the fractional area of sub-county j that spatially intersects an individual grid cell. In this way, county level emissions were scaled by the area overlap with the study area and emissions were attributed appropriately to grid cells that intersect multiple counties.

S4.7 Wetlands

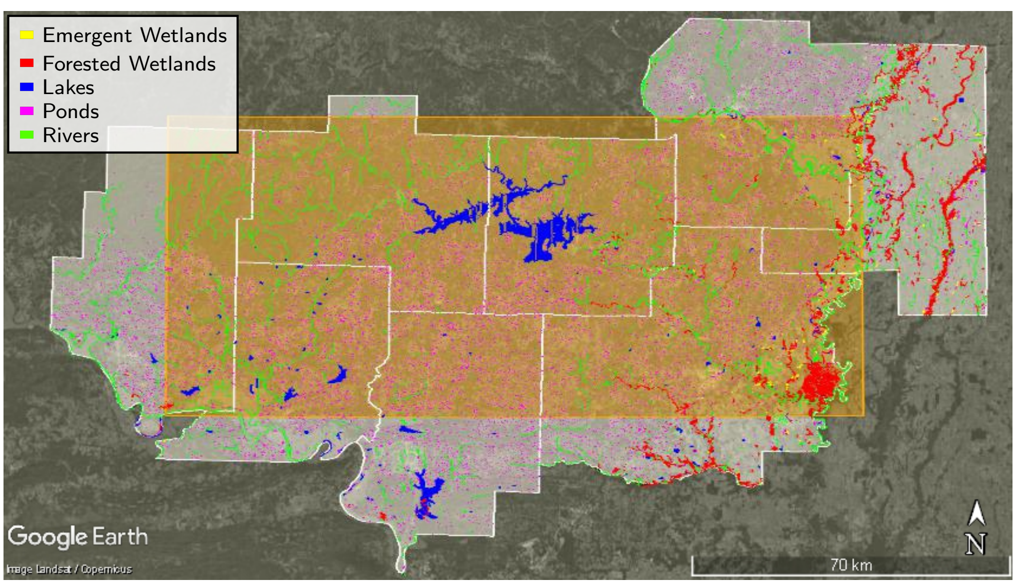

Figure S15: Wetlands considered within the study area.

Methane emissions from wetlands were calculated based on activity data from the U.S. Fish & Wildlife Service[25] and emission rates from a variety of sources. Geospatial data for land area containing permanently flooded emergent and forested wetlands, lakes, ponds and rivers were extracted from shapefiles downloaded from the national wetlands inventory.[25] Temporarily and seasonally flooded areas were not considered because the mass balance flights occurred during the dry season, on clear days during a period of little rainfall.

Table S11: Central, lower and upper bounds for triangular distributions used in wetland emission factor simulations.

Wetland Emission Rates Used In Model

Category	Central Estimate (kg/hr/m^2)	Lower Bound (kg/hr/m^2)	Upper Bound (kg/hr/m^2)
Forested Wetlands	3.75×10^{-6}	1.7×10^{-6}	6.7×10^{-6}
Emergent Wetlands	6.7×10^{-6}	4.25×10^{-6}	10.8×10^{-6}
Lakes	1.04×10^{-6}	1.0×10^{-6}	4.7×10^{-6}
Ponds	0.76×10^{-6}	0.4×10^{-6}	1.1×10^{-6}
Rivers	0.55×10^{-6}	-2.8×10^{-6}	3.9×10^{-6}

A range of emission rates for temperate and subtropical forested and emergent wetlands were obtained from Bartlett et al.[26] Deemer et al.[27] show that CH_4 emission rates are correlated with chlorophyll a concentrations. Chlorophyll a concentration measurements for Greers Ferry lake, the largest within the study area, were obtained from the Arkansas Department of Environmental Quality (ADEQ)[28]. A central estimate for CH_4 emission rates from lakes within the study area was made by comparing the chlorophyll a concentrations in Greers Ferry lake with the range of CH_4 concentrations and fluxes in Deemer et al., as described in Pickering.[19]

A recent study by Holgerson and Raymond[29] found that CH_4 fluxes from small ponds increased with decreasing surface area. They provide CH_4 flux rates for lakes and ponds of varying size class. The central estimate used in the model is a weighted average of these flux rates and the size class of all ponds within the study area. The lower and upper bounds are a weighted average of their reported standard error, expanded to two sigma.

Methane emissions rates for rivers in the study area were based on total CH_4 emissions, and total surface area for rivers located between 25°–54° latitude provided in Bastviken et al.[30] Lower and upper bounds were estimated by expanding their stated uncertainty on total CH_4 emissions to two sigma.

For each Monte Carlo iteration, i, CH_4 emissions from wetland category k are calculated as follows:

$$\dot{m}_{wetland(k),i} = \text{draw}(EF_k) \cdot (AD_k) \tag{9}$$

Where:

draw(EF_k) indicates drawing one emission factor value at random from a triangular distribution centered at EF_k, with associated lower and upper bounds as shown in Table S11

AD_k indicates the activity data (surface area) for grid cell m within the study area

Emissions for each wetland category were assumed to be distributed uniformly throughout each containing grid cell. Total surface area for each wetland category within each grid cell is calculated directly by spatial intersection. No intermediate allocation from county level to study area is required as was for livestock and rice cultivation.

S4.8 Geologic Seeps

Methane emissions from geologic seeps were calculated based on microseepage rates observed by Etiope et al.[31] Microseepage refers to positive CH_4 flux at the ground surface due to gas migration from underground gas reservoirs, which can potentially occur in sedimentary basins in dry climates with underlying gas or petroleum reservoirs.[31] Microseepage emission rates were categorized in three levels by Etiope et al. Level 1 seepage exceeds 50 mg/m^2/day, level 2 seepage ranges from 5–50 mg/m^2/day, and level 3 seepage ranges from 0–5 mg/m^2/day. In this study, the mean, lower and upper bounds for level 3 seepage were applied to the study area.

Table S12: Central, lower and upper bounds for triangular distributions used in geologic seep emission factor simulations.

Geologic Seep Emission Rates Used In Model

Category	Central Estimate (kg/hr/m^2)	Lower Bound (kg/hr/m^2)	Upper Bound (kg/hr/m^2)
Microseepage[a]	58×10^{-9}	0	208×10^{-9}

[a] Corresponds to level 3 seepage in Etiope et al.[31]

For each Monte Carlo iteration, i, CH_4 emissions from geologic seeps were calculated as follows:

$$\dot{m}_{seep,i} = \text{draw}(EF_{seep}) \cdot (AD_{seep}) \tag{10}$$

Where:

draw(EF_{seep}) indicates drawing one emission factor value at random from a triangular distribution centered at EF_{seep}, with associated lower and upper bounds as shown in Table S12

AD_{seep} indicates the activity data (surface area) for grid cell m within the study area

Calculated geologic seep emission were apportioned uniformly to study area grid cells.

S4.9 Landfills

Methane emissions from landfills were based on six measurements of landfills made by the aircraft during the field campaign, one of which was measured twice. The five measured landfills were not within the study area boundary, but were reported to the GHGRP. Measured rates and 95% confidence intervals are shown in Table S13, along with hourly rates calculated from annual CH_4 emission reported to GHGRP. Landfill areas were estimated using Google Earth, and emission factors were created based on the rate measured by the aircraft, and the estimated area. The study area only contained one landfill to the authors' knowledge, and this landfill was not reported to the GHGRP. The area of the landfill was also estimated using Google Earth, and the developed emission factors were applied in the Monte Carlo Model as follows.

For each Monte Carlo iteration, i, CH_4 emissions from the landfill were calculated as follows:

$$\dot{m}_{landfill,i} = \text{draw}(EF_{landfill}) \cdot (AD_{landfill}) \tag{11}$$

Where:

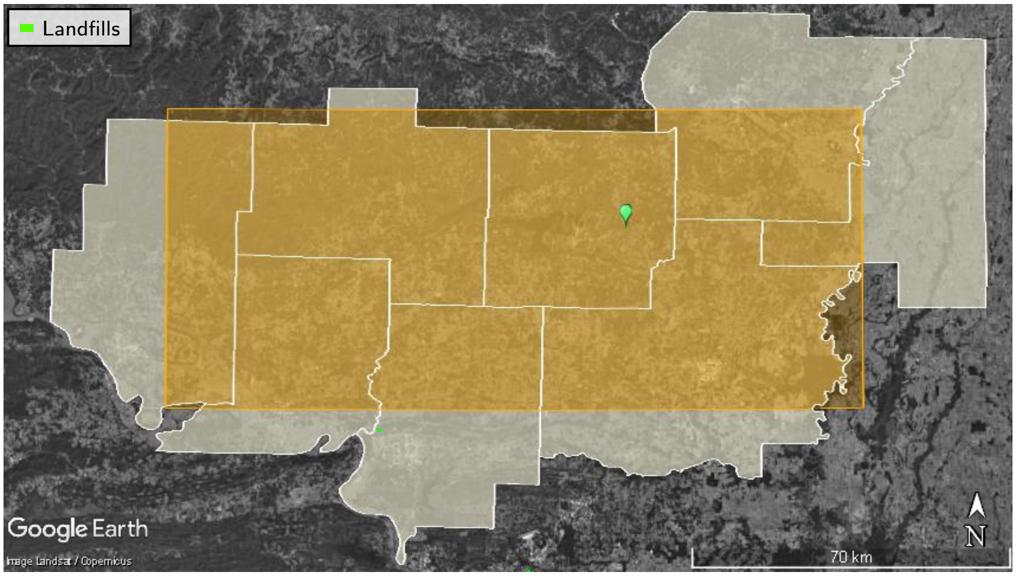

Figure S16: Only one landfill (green balloon) was identified within the study area (orange highlighting).

Table S13: Landfill emission factors measured by aircraft compared to GHGRP reported average rates. Areas were estimated using Google Earth.

Landfill	Date	Aircraft Estimate (kg/h)	GHGRP (kg/h)	Area (m^2)	Study EF (kg/h/m^2)
Conway	9/25/2015	251.1±59.6	627.0	444 920	5.64×10^{-4}
Conway	10/13/2015	263.9±37.8	627.0	444 920	5.93×10^{-4}
Little Rock City	10/13/2015	1105.6±141.6	172.2	649 973	1.70×10^{-3}
Modelfill	10/13/2015	18±2.3	35.2	558 079	3.23×10^{-5}
Two Pine	10/13/2015	788±177	277.5	1 168 453	6.74×10^{-4}
Saline	10/13/2015	441.9±107	627.0	437 173	1.01×10^{-3}

draw($EF_{landfill}$) indicates drawing one emission rate at random from the six landfill measurements made in the study. Uncertainty is then considered drawing a new emission rate from a triangular distribution centered at the measured emission rate drawn, and bounded by its associated confidence interval, as shown in Table S13. This emission rate is then normalized by the estimated area of the measured landfill resulting in $EF_{landfill}$

$AD_{landfill}$ indicates the activity data (surface area) for the simulated landfill

Calculated emissions were then assigned to the landfill category in the grid cell that contains the landfill.

S4.10 Wastewater Treatment

Methane emissions from wastewater treatment were based on 2015 population estimates for study area counties from the U.S. Census[32], and septic usage estimates from the National Environmental Services Center[33]. Sewer and septic use were provided on a per household basis and we have assumed an equivalent ratio on a per person basis.

Table S14: Wastewater activity data used in the model.

Modeled County-Level Activity Data

County	Population	Households with Central Sewer (%)	Households with Septic Systems (%)
Cleburne	25 467	29	68
Conway	21 019	40	58
Faulkner	121 552	49	50
Independence	12 898	35	64
Jackson	17 338	63	35
Pope	63 390	51	48
Van Buren	16 771	25	70
White	79 161	51	48

* A portion of households in each county are served by other means

Emission factors were developed from a study on residential septic systems by Leverenz et al.[34], and from the GHGI[21] for centralized sewer systems. The GHGI estimates that 80% of the U.S. population is served by centralized sewer systems. Total CH_4 emissions from sewer system were divided by 80% of the U.S. population resulting in an emission factor of 1.3 g CH_4/day/person. Uncertainty was assumed to be the same as that provided for residential wastewater treatment, -37% / +8%.

Table S15: Wastewater emission factors used in the model.

Wastewater Emission Rates Used In Model

Category	Central Estimate (g/day/person)	Lower Bound (g/day/person)	Upper Bound (g/day/person)
Septic Tanks[a]	11.0	6.3	17.9
Sewer Systems[b]	1.3	0.8	1.4

[a] Central estimate is geometric mean of all sampled septic tanks. Upper and lower bounds are the geometric means of multiple measurements of individual tanks.[34]

[b] Estimated from US Census and GHGI

For each Monte Carlo iteration, i, CH_4 emissions from wastewater treatment in county j were calculated as follows:

$$\dot{m}_{wastewater,i} = \text{draw}(EF_{sewer}) \cdot (AD_{sewer}) + \text{draw}(EF_{septic}) \cdot (AD_{septic}) \tag{12}$$

Where:

draw(EF_{sewer}) or draw(EF_{septic}) indicates drawing one emission factor value at random from a triangular distribution centered at EF_{sewer} or EF_{septic}, and bounded by its associated confidence interval

AD_{sewer} or AD_{septic} indicates the activity data (sewer or septic users) for county j

Emissions were assumed to be distributed uniformly throughout the county area and were apportioned to grid cells in a two-step process. First, emissions from county j were scaled by the fractional area of county j that spatially intersects the study area, resulting in a sub-county emission estimate. Second, sub-county emissions were apportioned to grid cells by the fractional area of sub-county j that spatially intersects an individual grid cell. In this way, county level emissions were scaled by the area overlap with the study area and emissions were attributed appropriately to grid cells that intersect multiple counties.

S4.11 GHGRP Facilities

Facilities reporting to the EPA GHGRP in categories other than Petroleum and Natural Gas Systems were identified using the EPA Facility Level Information on GreenHouse gases Tool (FLIGHT)[35]. Only one facility within the study area was identified which was not accounted for in other categories within the model.

Table S16: GHGRP Facility emission factors used in the model.

GHGRP Facility Emission Rates Used In Model

Facility	Reported Methane Emissions (tonne CH_4/yr in CO_2e)	Modeled Methane Emissions (kg CH_4/hr)[a]
Independence Power Plant	14 662	66.9

[a] AR4 GWPs

For each Monte Carlo iteration, i, CH_4 emissions from GHGRP facilities, were calculated from reported methane emissions in tonne CH_4/yr $CO2_e$, assuming IPCC fourth assessment report global warming potentials (GWPs), and 8,760 hrs. Emissions were assumed constant, and no uncertainty was applied. Emissions were assigned spatially to the GHGRP category in the grid cells that contain the facilities.

S5 Emission Factor Accuracy and Applicability: Temporal Variation During Aircraft Transects on October 1st

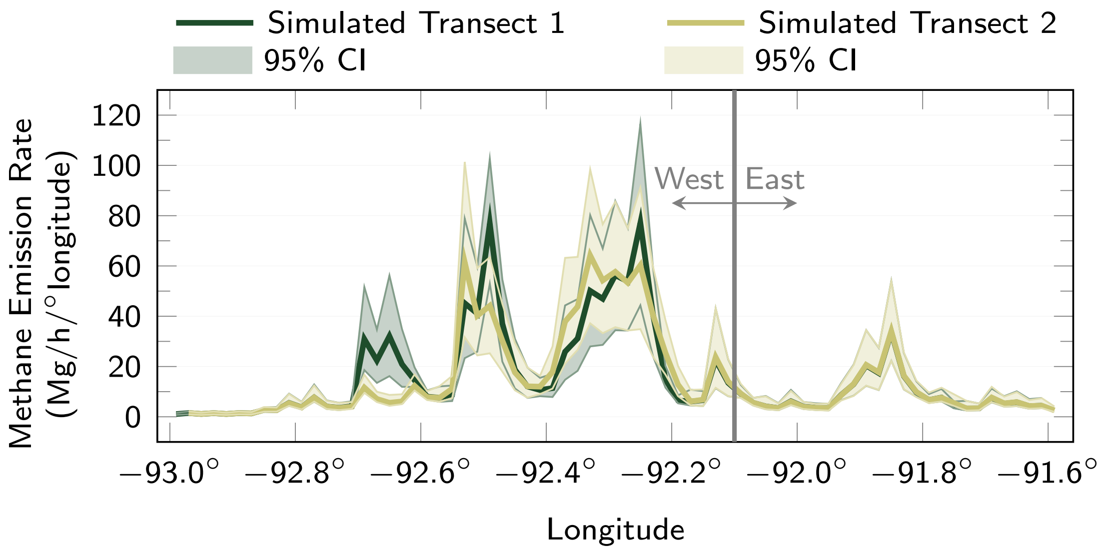

Figure S17: Simulated BU longitudinal emission rate profiles corresponding to individual TD aircraft transects made on October 1st. Study partner provided activity data indicates an emission source at -92.7° longitude that was active during the first aircraft transect, but inactive during the second.

S6 List of Abbreviations

ADEQ Arkansas Department of Environmental Quality

CH_4 methane

EPA Environmental Protection Agency

FLIGHT Facility Level Information on GreenHouse gases Tool

GHGI greenhouse gas inventory

GHGRP greenhouse gas reporting program

GLAE ground-level area estimate

GWP global warming potential

IPCC Intergovernmental Panel on Climate Change

MLU manual liquid unloading

M&R metering and regulating

ODM on-site direct measurement

OGI optical gas imaging

SDM simulated direct measurement

SOE study on-site estimate

TDTS transmission distribution transfer station

USDA United States Department of Agriculture

References

1. Allen, D. T. *et al.* Methane Emissions from Process Equipment at Natural Gas Production Sites in the United States: Liquid Unloadings. *Environmental Science & Technology* **49,** 641–648. ISSN: 0013-936X (Jan. 2015).
2. Bell, C. *et al.* Comparison of Methane Emission Estimates from Multiple Measurement Techniques at Natural Gas Production Pads. en. *Elem Sci Anth* **5.** ISSN: 2325-1026. doi:10.1525/elementa.266 (Dec. 2017).
3. Vaughn, T. L. *et al.* Comparing Facility-Level Methane Emission Rate Estimates at Natural Gas Gathering and Boosting Stations. en. *Elem Sci Anth* **5.** ISSN: 2325-1026. doi:10.1525/elementa.257 (Nov. 2017).
4. Zimmerle, D. J. *et al.* Gathering Pipeline Methane Emissions in Fayetteville Shale Pipelines and Scoping Guidelines for Future Pipeline Measurement Campaigns. en. *Elem Sci Anth* **5.** ISSN: 2325-1026. doi:10.1525/elementa.258 (Nov. 2017).
5. Yacovitch, T. I. *et al.* Natural Gas Facility Methane Emissions: Measurements by Tracer Flux Ratio in Two US Natural Gas Producing Basins. en. *Elem Sci Anth* **5.** ISSN: 2325-1026. doi:10.1525/elementa.251 (Nov. 2017).
6. US EPA, O. *GHG Reporting Program Data Sets* en. https://www.epa.gov/ ghgreporting/ghg-reporting-program-data-sets. Overviews and Factsheets. May 2015.
7. Schwietzke, S. *et al.* Improved Mechanistic Understanding of Natural Gas Methane Emissions from Spatially Resolved Aircraft Measurements. *Environmental Science & Technology* **51,** 7286–7294. ISSN: 0013-936X (June 2017).
8. Allen, D. T. *et al.* Measurements of Methane Emissions at Natural Gas Production Sites in the United States. en. *Proceedings of the National Academy of Sciences* **110,** 17768–17773. ISSN: 0027-8424, 1091-6490 (Oct. 2013).
9. Allen, D. T. *et al.* Methane Emissions from Process Equipment at Natural Gas Production Sites in the United States: Pneumatic Controllers. *Environmental Science & Technology* **49,** 633–640. ISSN: 0013-936X (Jan. 2015).
10. Bacharach, Inc. *HI FLOW® Sampler For Natural Gas Leak Rate Measurement* July 2015.
11. US EPA. *Method 19 - Sulfur Dioxide Removal and Particulate, Sulfur Dioxide and Nitrogen Oxides from Electric Utility Steam Generators* en. https://www.epa.gov/emc/method-19-sulfur-dioxide-removal-and-particulate-sulfur-dioxide-and-nitrogen-oxides-electric. Policies and Guidance.
12. US EPA. *Method 320 - Vapor Phase Organic and Inorganic Emissions by Extractive FTIR* en. https://www.epa.gov/emc/method-320-vapor-phase-organic-and-inorganic-emissions-extractive-ftir. Policies and Guidance.
13. Office of Air Quality Planning and Standards, U. E. *Emissions Factors & AP 42* en. http://www.epa.gov/ttn/chief/ap42/index.html.
14. Caterpillar. *Caterpillar Application & Installation Guide Crankcase Ventilation Systems* s7d2.scene7.com/is/ 53120-62603.

15. Myers, D. *Methane Emissions from the Natural Gas Industry, Volume 14: Glycol Dehydrators Final Report* tech. rep. EPA 600/R-96-080n (June 1996).
16. Conley, S. *et al.* Application of Gauss's Theorem to Quantify Localized Surface Emissions from Airborne Measurements of Wind and Trace Gases. *Atmos. Meas. Tech.* **10,** 3345–3358. ISSN: 1867-8548 (Sept. 2017).
17. 40 C.F.R. § 98.33. *MANDATORY GREENHOUSE GAS REPORTING Subpart C: General Stationary Fuel Combustion Sources* en-US.
18. 40 C.F.R. § 98.230. *MANDATORY GREENHOUSE GAS REPORTING Subpart W: Petroleum and Natural Gas Systems* en-US.
19. Pickering, C. *METHANE EMISSIONS FROM GATHERING PIPELINE NETWORKS, DISTRIBUTION SYSTEMS, AGRICULTURE, WASTE MANAGEMENT AND NATURAL SOURCES* Masters Thesis (Colorado State University, Fort Collins, CO, 2016).
20. GTI. *Field Measurement Program to Improve Uncertainties for Key Greenhouse Gas Emission Factors for Distribution Sources* tech. rep. OTD-10-0002 (Nov. 2009).
21. US EPA. *Inventory of U.S. Greenhouse Gas Emissions and Sinks: 1990-2014* tech. rep. (Washington, D.C., Apr. 2016).
22. IPCC 2006. *2006 IPCC Guidelines for National Greenhouse Gas Inventories, Prepared by the National Greenhouse Gas Inventories Programme* (eds Eggleston H.S., Buendia L., Miwa K., Ngara T. & Tanabe K.) 2006.
23. *USDA - NASS, Census of Agriculture - 2012 Census Volume 1, Chapter 2: County Level Data* https://www.agcensus.usda.gov/Publications/2012/Full_Report/Volume_1,_Chapter_2_County_Level/Arkansas/.
24. Smartt, A. D. *et al.* Chamber Size Effects on Methane Emissions from Rice Production. *Open Journal of Soil Science* **05,** 227–235. ISSN: 2162-5360, 2162-5379 (2015).
25. U.S. Fish & Wildlife Service. *National Wetlands Inventory: State Downloads* https://www.fws.gov/wetlands Downloads.html.
26. Bartlett, K. B., Crill, P. M., Bonassi, J. A., Richey, J. E. & Harriss, R. C. Methane Flux from the Amazon River Floodplain: Emissions during Rising Water. en. *Journal of Geophysical Research: Atmospheres* **95,** 16773–16788. ISSN: 2156-2202 (Sept. 1990).
27. Deemer, B. R. *et al.* Greenhouse Gas Emissions from Reservoir Water Surfaces: A New Global Synthesis. *BioScience* **66,** 949–964. ISSN: 0006-3568 (Nov. 2016).
28. *Water Quality Monitoring Data — ADEQ* https://www.adeq.state.ar.us/techsvs/env_multi_lab/water_quality_station.aspx.
29. Holgerson, M. A. & Raymond, P. A. Large Contribution to Inland Water CO2 and CH4 Emissions from Very Small Ponds. en. *Nature Geoscience* **9,** 222–226. ISSN: 1752-0894 (Mar. 2016).
30. Bastviken, D., Tranvik, L. J., Downing, J. A., Crill, P. M. & Enrich-Prast, A. Freshwater Methane Emissions Offset the Continental Carbon Sink. en. *Science* **331,** 50–50. ISSN: 0036-8075, 1095-9203 (Jan. 2011).

31. Etiope, G. & Klusman, R. W. Microseepage in Drylands: Flux and Implications in the Global Atmospheric Source/Sink Budget of Methane. *Global and Planetary Change. Quaternary and Global Change: Review and Issues Special issue in memory of Hugues FAURE* **72,** 265–274. ISSN: 0921-8181 (July 2010).

32. *Population Estimates, July 1, 2016, (V2016)* //www.census.gov/quickfacts/.

33. *Integrated Database: Arkansas Sewer Data* http://www.nesc.wvu.edu/septic_idb/arkansas.htm#septicstats

34. Leverenz, H. L., Tchobanoglous, G. & Darby, J. *Evaluation of Greenhouse Gas Emissions from Septic Systems* OCLC: ocn890654374. ISBN: 978-1-84339-616-1 (Water Environment Research Foundation ; IWA Publishing, Alexandria, VA : London, UK, 2010).

35. *EPA Facility Level GHG Emissions Data* http://ghgdata.epa.gov/ghgp/main.do.